Check for updates

Hydrothermal synthesis of high surface area CuCrO$_2$ for H$_2$ production by methanol steam reforming†

Rong-Jun Huang,[a] Subramanian Sakthinathan,[a] Te-Wei Chiu [iD] *[a] and Chaofang Dong [iD] *[b]

Hydrogen (H$_2$) is viewed as an alternative source of renewable energy in response to the worldwide energy crisis and climate change. In industry, hydrogen production is mainly achieved through steam reforming of fossil fuels. In this research, hydrothermally-synthesized delafossite CuCrO$_2$ nanopowder were applied in methanol steam reforming. Reducing the size of the CuCrO$_2$ nanopowder significantly improved the efficiency of hydrogen production. The prepared CuCrO$_2$ nanopowder were characterized by X-ray diffraction, Brunauer–Emmett–Teller (BET) analysis, field emission scanning electron microscopy, and transmission electron microscopy. The calculated BET surface area of the hydrothermally synthesized CuCrO$_2$ nanopowder was 148.44 m^2 g^{-1}. The CuCrO$_2$ nanopowder displayed high catalytic activity, and the production rate was 2525 mL STP per min per g-cat at 400 °C and a flow rate of 30 sccm. The high specific area and steam reforming mechanism of the CuCrO$_2$ nanopowder catalyst could have vital industrial and economic effects.
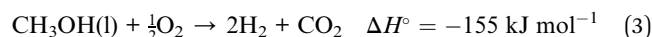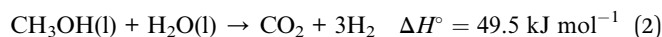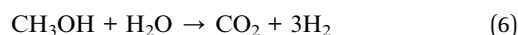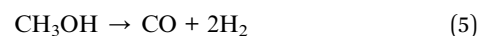
1. Introduction

To address climate change and the limited supply of fossil fuels, alternative sources of energy have been considered.[1] Hydrogen fuel cell applications are a promising technology, for unlike fossil fuels, hydrogen (H$_2$) burns cleanly and emits no environmental pollutants.[2] Furthermore, as compared with other fuels, H$_2$ also has the highest energy density per unit weight (*i.e.*, 120.7 kJ g^{-1}).[3] Today, industrial hydrogen is mainly produced by steam reforming. One source of liquid hydrogen is methanol, which is superior to fuels such as ethanol, gasoline, and diesel.[4] Methanol has a higher H$_2$/C ratio than that of ethanol, which allows it to be reformed at a relatively lower temperature. It also lacks a carbon–carbon bond, is low in sulfur compounds (<5 ppm), and yields a smaller quantity of carbonaceous products.[5] Generally, hydrogen is produced from methanol by reactions such as decomposition,[6] methanol steam reforming (MSR), and partial oxidation, which are described in the following chemical reactions.[7]

$$CH_3OH(l) \rightarrow 2H_2 + CO \quad \Delta H° = 92.0 \text{ kJ mol}^{-1} \quad (1)$$

$$CH_3OH(l) + H_2O(l) \rightarrow CO_2 + 3H_2 \quad \Delta H° = 49.5 \text{ kJ mol}^{-1} \quad (2)$$

$$CH_3OH(l) + \tfrac{1}{2}O_2 \rightarrow 2H_2 + CO_2 \quad \Delta H° = -155 \text{ kJ mol}^{-1} \quad (3)$$

The decomposition reaction produces a high amount of CO, which can damage the electrode and decrease the power density of fuel cells, so it is not an ideal process for fuel cells.[8] The steam reforming reaction is endothermic, making it ideal for fuel cell applications, but it produces a large amount of carbon dioxide as a byproduct. Partial oxidation is a strongly exothermic reaction that can provide rapid reaction requirements for vehicles, but its hydrogen production rate is only 66%, which is less efficient than that of steam reforming, and the reaction temperature is difficult to control.[9] In contrast, steam reforming is an efficient and advantageous method of producing hydrogen. The design of the fuel cell processor will require a catalytic reformer that is fast, highly active, compact, and light in weight.[10]

Traditionally, hydrogen has been converted by SRM with the following reactions: (4) water gas shift (WGS), (5) methanol decomposition, and (6) steam reforming of methanol (SRM).

$$CO + H_2O \rightarrow CO_2 + H_2 \quad (4)$$

$$CH_3OH \rightarrow CO + 2H_2 \quad (5)$$

$$CH_3OH + H_2O \rightarrow CO_2 + 3H_2 \quad (6)$$

The SRM process has received great interest as a method of producing hydrogen due to its low reaction temperature, acceptable water miscibility, high ratio of hydrogen

[a]*Department of Materials and Mineral Resources Engineering, National Taipei University of Technology, 1, Section 3, Zhongxiao E. Rd, Taipei 106, Taiwan. E-mail: tewei@ntut.edu.tw*

[b]*Corrosion and Protection Center, Key Laboratory for Corrosion and Protection (MOE), University of Science and Technology, Beijing, China. E-mail: cfdong@ustb.edu.cn*

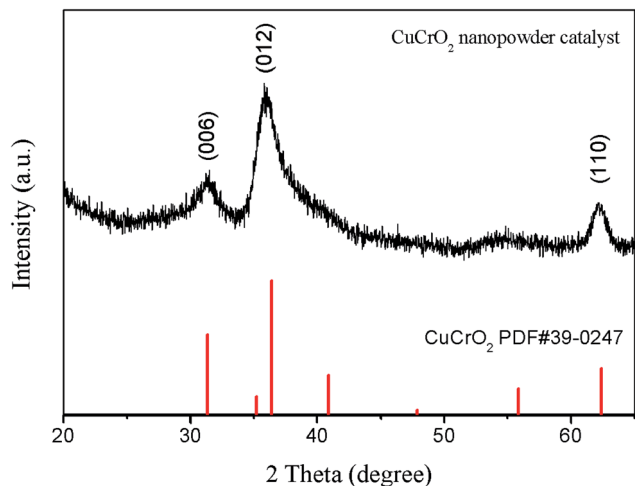† Electronic supplementary information (ESI) available. See DOI: 10.1039/d1ra01332g

Fig. 1 The XRD pattern of CuCrO$_2$ nanopowder prepared by hydrothermal method.

concentration, and low CO level. Also, SRM is a simple, efficient endothermic reaction, which makes it suitable for fuel cell applications.[11,12]

Generally, catalysts comprising Cu, Pd, Ru, Zn, Ni, or combinations of these metals are used in the SRM reaction. The reaction conditions and the catalyst synthesis processes greatly influence the effectiveness of methanol steam reforming in a reactor.[13] In particular, metal oxide and copper-based catalysts, such as Al$_2$O$_3$,[14] ZnO/Al$_2$O$_3$, ZrO$_2$/Al$_2$O,[15] CuO/ZnO/Al$_2$O,[16] Cr$_2$O$_3$/Al$_2$O$_3$,[17] and Cu/ZnO/Al$_2$O$_3$/CeO$_2$/ZrO$_2$,[5] are used for SRM. These aforementioned catalysts have received a lot of attention in hydrogen production due to their high activity

and selectivity.[18] However, the main problem with the SRM process is the accumulation of carbon particles on the surface of the Cu-related catalyst, as they reduce the performance of the catalyst.[19] To improve the catalytic efficiency, the scattering of copper particles on the surface must be homogeneous, so to improve the catalytic performance, numerous researchers have combined copper-based catalysts with metal oxides, such as ZnO,[20] Fe$_2$O$_3$,[21] Cr$_2$O$_3$,[22] and CoO.[23] The Cu-related catalyst prepared from delafossite (CuCrO$_2$) has good dispersion of copper nanoparticles and high thermal stability.[24] In addition, one of the most widely used techniques for the preparation of delafossite CuCrO$_2$ is hydrothermal synthesis. The hydrothermal method has several advantages, such as the use of water as a solvent and the synthesis of well-crystallized materials, the crystal size and morphology can be controlled.[25,26] Hence, in this study, CuCrO$_2$ nanopowder was synthesized by hydrothermal method. The prepared CuCrO$_2$ nanopowder was expected to have a high response for use in SRM because of its high surface area. The CuCrO$_2$ nanopowder was employed in an adiabatic fixed-bed reactor for the steam reforming of methanol, and the reduction activity was investigated. Also, at various operating temperatures, the hydrogen output rate of the CuCrO$_2$ nanopowder was compared with those of commercial and previously-reported catalysts.

2. Experimental procedure

2.1 Formation of CuCrO$_2$ nanopowder by hydrothermal method

For the preparation of the CuCrO$_2$ nanopowder by hydrothermal method, the starting reagents of chromium nitrate

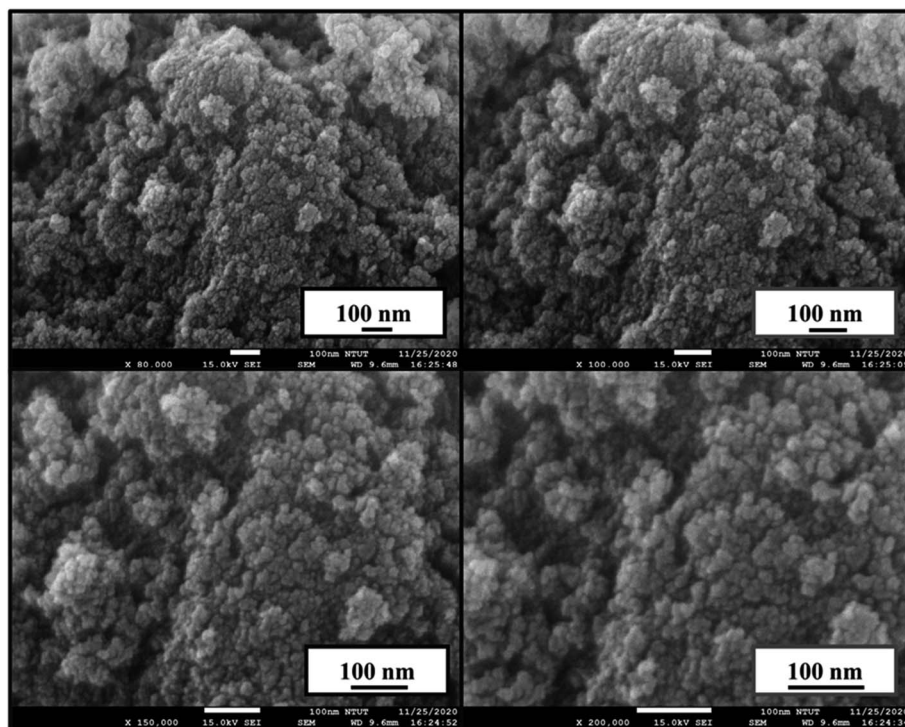Fig. 2 Morphology of CuCrO$_2$ nanopowder prepared by hydrothermal method.

($Cr(NO_3)_3 \cdot 9H_2O$), copper(II) nitrate ($Cu(NO_3)_2 \cdot 3H_2O$), and NaOH were acquired from Sigma-Aldrich, Taiwan. In this experiment, all reagents were analytical grade and used without further purification. Generally, 2.6 mmol $Cr(NO_3)_3 \cdot 9H_2O$ and 2.6 mmol $Cu(NO_3)_2 \cdot 3H_2O$ were dissolved in 35 mL DI water with homogeneous stirring, and 0.8625 g NaOH was added as a mineralizer. Then the obtained solution was transferred to a Teflon-lined autoclave (50 mL), which was sealed before being held at 240 °C for 60 h. The resulting dark green precipitate was washed several times with DI water. Finally, the obtained $CuCrO_2$ nanopowder was dried and stored in a sample bottle for further use.

2.2 Characterization

The following methods were used to identify the prepared Cu-based catalyst. The crystalline phases of the nanopowders were identified by X-ray diffraction (XRD) (D2 Phaser, Bruker) with Cu Kα radiation ($\lambda = 0.15418$ nm), a working voltage of 30 kV, and working current of 10 mA. After the diffraction studies, the obtained data were analyzed in MDI JADE 5.0 software and compared with the JCPDS card database. Scanning electron microscopy (FE-SEM, JEOL, JSM-7610F) was used to observe the surface morphology of the nanopowder. The working voltage was 30 kV and the working power was 10 mA. The particle size and morphology were identified by transmission electron microscopy

(TEM) (Japan Electron Optic Co. Ltd., JEOLTM, JEM-2100F, Tokyo, Japan) at an operating voltage of 200 kV and pressure of 10^{-8} Pa. The surface area of the $CuCrO_2$ nanopowder (S_{BET}) was investigated by Brunauer–Emmett–Teller (BET) analysis.

2.3 Catalyst test

At atmospheric pressure, the prepared catalyst was placed in a reactor and used for the SRM process. In each experiment, 0.04 g of catalyst was loaded into a tubular reactor. The SRM experiment was conducted in a flow reactor connected with a 25 cm quartz pipe having an inner diameter of 1.2 cm. The rate of hydrogen production was analyzed by gas chromatography (GC 1000 China Chromatography TCD) with one column (60/80 Carboxen® 1000) for H_2 (7 ft × 1/8 in, stainless steel). The gas chromatograph was equipped with a thermal conductivity detector (TCD) with a current of 50 mA. Nitrogen was used as the dilutant and carrier gas at a flow rate of 30 sccm. The gas from the outlet tube was analyzed with a gas chromatograph several times at each temperature to analyze the hydrogen production rate (mL STP per min per g-cat) and the catalytic efficiency of the $CuCrO_2$.

$$\text{Methanol conversion } (\%) = \frac{(\text{methanol})_{in} - (\text{methanol})_{out}}{(\text{methanol})_{in}} \times 100 \quad (7)$$
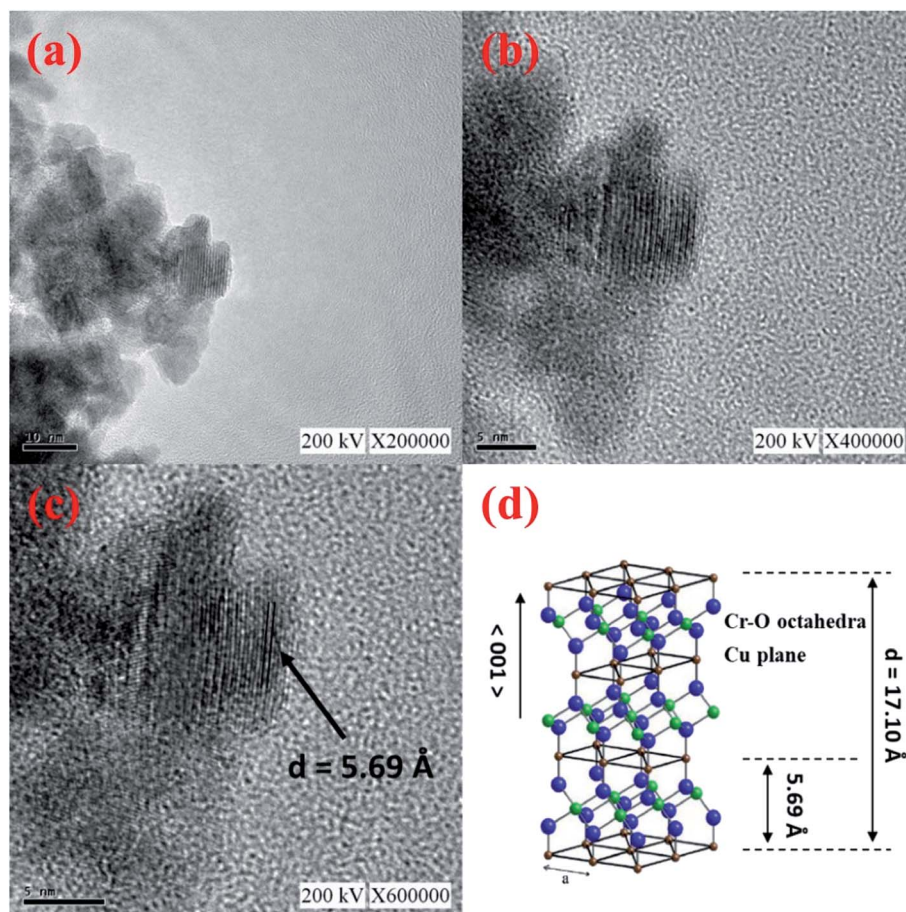

Fig. 3 (a–c) TEM images of the $CuCrO_2$ nanopowder prepared by hydrothermal method; (d) crystalline structure of $CuCrO_2$ nanopowder.

$$\text{Hydrogen production rate} = \frac{H_2\% \text{ mL } 30 \text{ mL/min}}{cm^3 \text{ g}} \quad (8)$$

The subscript "out" indicates the total outlet flow rate of each species, while "in" refers to the feed source in the above equations for measuring methanol conversion.[27,28]

3. Results and analysis

3.1 XRD analysis

The crystal structures of the $CuCrO_2$ nanopowder catalysts were studied by XRD and analyzed with powder X-ray diffractometric tools. Fig. 1 presents the XRD pattern of $CuCrO_2$ nanopowder prepared by the hydrothermal method. The XRD pattern of the $CuCrO_2$ nanopowder (JCPDF card no. 39-0247) shows three main reflections for the (006), (012), and (110) planes. It is apparent that the $CuCrO_2$ delafossite structure was obtained.

3.2 SEM and TEM analysis

The morphology of the hydrothermally-synthesized $CuCrO_2$ nanopowder was identified by SEM studies and is presented in Fig. 2. The nanopowder consisted of small nanocrystals of similar morphology, and the size of the $CuCrO_2$ nanoparticles was further verified by TEM.

The structure of the $CuCrO_2$ nanopowder was further confirmed by TEM. The TEM images of the $CuCrO_2$ nanopowder are shown in Fig. 3(a–c). Fig. 3(c) shows $CuCrO_2$ interplates with a cross-section plane spacing of 5.69 Å. The distance along the c-axis (the $\langle 001 \rangle$ direction) of the delafossite structure is illustrated in Fig. 3(d). The particle size of the $CuCrO_2$ nanopowder was 5–10 nm, which resulted in a high surface area.

3.3 TEM-EDS analysis

The elemental composition and arrangement of the $CuCrO_2$ nanopowder were analyzed by TEM-EDS mapping, and the results are shown in Fig. 4. As can be seen in Fig. 4(a), the elements Cu, Cr, and O were all present. The elemental

Table 1 The surface areas of $CuCrO_2$ nanopowders synthesized by hydrothermal method, GNP method, and solid-state method

Method	Surface area (m^2 g^{-1})
Hydrothermal	148
GNP (ref. 10)	28.5
Solid-state (ref. 13)	0.47
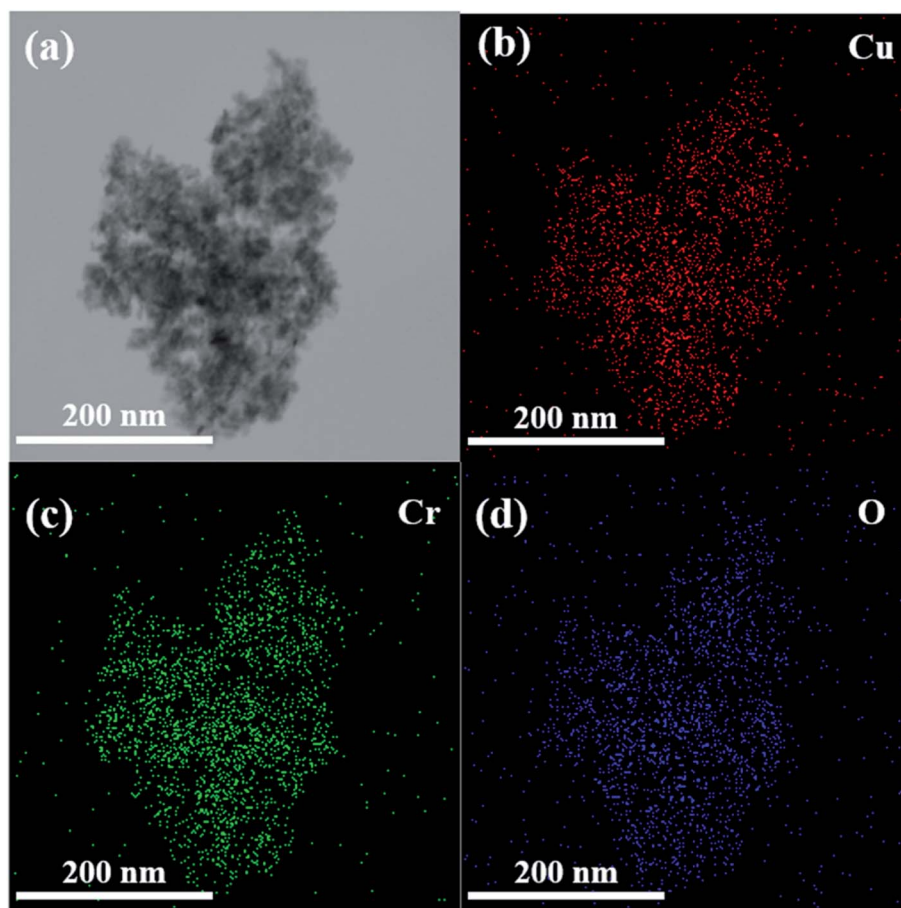
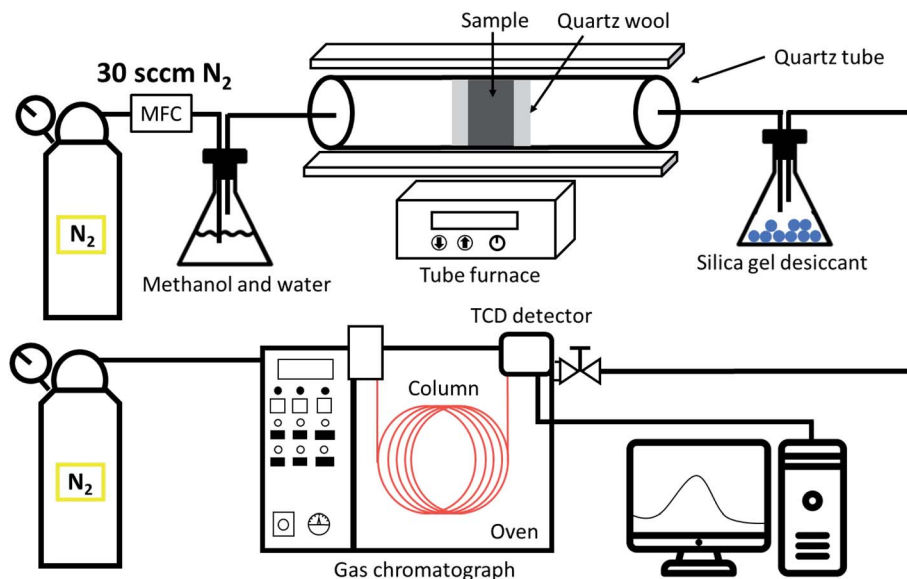Fig. 4 (a–d) TEM-EDS elemental distributions of the $CuCrO_2$ nanopowder synthesized by hydrothermal method.

Fig. 5 Schematic diagram of the CuCrO$_2$ nanopowder catalytic test in the methanol steam reforming process.

arrangement mapping signals of (Fig. 4(b)) Cu, (Fig. 4(c)) Cr, and (Fig. 4(d)) O showed uniform distribution within the small nanoparticles of the CuCrO$_2$ nanopowder. Moreover, the effective formation of the CuCrO$_2$ nanopowder was confirmed by the TEM-EDS analysis.

3.4 BET analysis

The surface area of the hydrothermally-synthesized CuCrO$_2$ nanopowder was studied by BET methods. After the nanopowder was degassed at 150 °C for 6 hours, high purity nitrogen gas was passed through the CuCrO$_2$ nanopowder to eliminate any adsorbed water. For measurement, the sample tube was filled with high purity nitrogen gas, and then the dried CuCrO$_2$ nanopowder adsorbed nitrogen at −196 °C. A relative pressure variable $P/P_0 = 0$–0.3 was used to determine the volume of nitrogen adsorption. The BET measurement showed that the surface area of the hydrothermally-synthesized CuCrO$_2$ nanopowder was 148 m^2 g^{-1}. The specific surface area of the nanopowder was compared with those of CuCrO$_2$ prepared by GNP[29] and solid-state[30] methods. The comparison studies showed that the hydrothermally-prepared CuCrO$_2$ nanopowder exhibited a higher surface area than those of the other two materials, and the results are listed in Table 1.

3.5 Production of hydrogen from methanol by steam reforming process

The rate of H$_2$ production was measured with a gas chromatograph equipped with a thermal conductivity detector, and 0.04 g of catalyst was used for this study (Fig. 5). The hydrogen efficiency and productivity at a flow rate of 30 sccm were measured at 250–400 °C (ESI Fig. 1–4†) and converted to milliliters per minute (mL STP per min per g-cat). The temperature of the methanol and water was 80 °C, and the ratio of methanol to water was 1 : 4 due to the vapor pressure difference. For

maximum yield, the CuCrO$_2$ nanoparticle catalyst powder was activated at each temperature for 10 min without contact with the methanol steam. Then the carrier gas was turned on to fill the system with methanol steam and detection was performed at the gas outlet pipe.

Fig. 6 presents the relationship between the production rate of H$_2$ and the reaction temperature in the methanol steam reforming process performed with the CuCrO$_2$ nanopowder
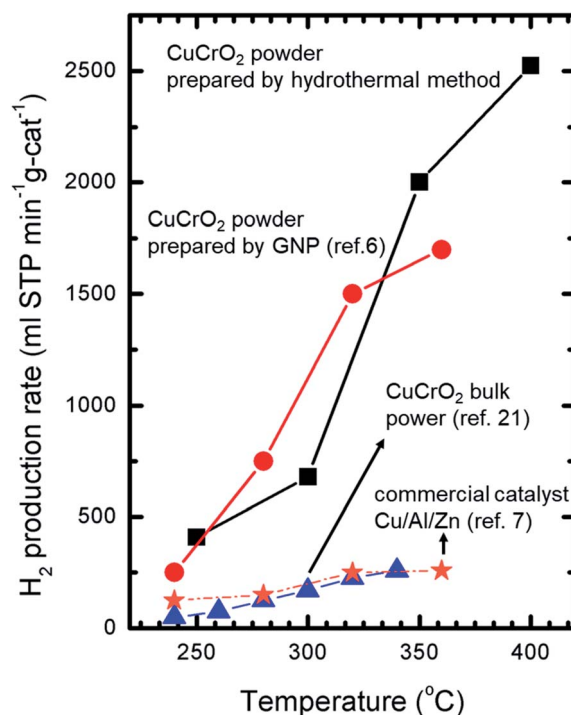

Fig. 6 The H$_2$ production rate *versus* reaction temperatures in the SRM process.

catalyst. The maximum hydrogen production rate was 2525 mL STP per min per g-cat at 400 °C. The H_2 production performances of the hydrothermally-synthesized $CuCrO_2$ nanopowder catalyst, commercial Cu/Al/Zn catalyst and $CuCrO_2$ bulk catalyst[31] are compared in Fig. 6. The comparison showed that the hydrogen production efficiency of the hydrothermally-synthesized $CuCrO_2$ nanopowder was much higher than those of the $CuCrO_2$ nanopowder catalysts prepared by GNP method,[6] commercial Cu/Al/Zn catalyst,[23] and $CuCrO_2$ bulk power catalyst.[29] Commonly, a H_2-activated catalyst is dangerous when exposed to air due to its high activity and potential for ignition and explosion, but $CuCrO_2$ nanopowder is very stable in air. There was thus no need for high-temperature activation treatment of the $CuCrO_2$ nanopowder catalyst for the SRM process. This finding suggests that, if $CuCrO_2$ nanopowder is installed in a fuel cell vehicle, higher efficiency can be achieved than with conventional catalysts.[6] In future work, the stability of the catalyst, SRM conditions, and optimization of reactor conditions will be tested.

4. Conclusion

$CuCrO_2$ nanopowder was prepared by hydrothermal method and applied to SRM. The $CuCrO_2$ nanopowder was verified by XRD, BET analysis, FE-SEM, and TEM studies. Furthermore, the high surface area of the $CuCrO_2$ catalyst (148.44 m^2 g^{-1}) was suitable, and the catalyst was applied for SRM catalysis. The specific surface area of the $CuCrO_2$ nanopowder was influenced by the SRM process. This catalyst was used to produce hydrogen by steam reforming of methanol in a bed reactor at temperatures of 230 to 400 °C. The maximum hydrogen generation rate was 2525 mL STP per min per g-cat at 400 °C, and the catalyst could be activated without a high temperature, making it suitable for installation in fuel cell vehicles. Furthermore, the stability of the catalyst and the reactor conditions for SRM were studied. The hydrogen generation rate of the $CuCrO_2$ nanopowder was compared with those of commercial and previously-reported catalysts under the same operating conditions. The results indicated that this hydrothermally-synthesized $CuCrO_2$ nanopowder is suitable for H_2 production and fuel cell application.

Conflicts of interest

There are no conflicts of interest to declare.

Acknowledgements

References

1 M. Hook and X. Tang, Depletion of fossil fuels and anthropogenic climate change-a review, *Energy Policy*, 2013, **52**, 797–809.

2 B. Lindström and L. J. Pettersson, Hydrogen generation by steam reforming of methanol over copper-based catalysts for fuel cell applications, *Int. J. Hydrogen Energy*, 2001, **26**, 923–933.

3 A. Haryanto, S. Fernando, N. Murali and S. Adhikari, Current status of hydrogen production techniques by steam reforming of ethanol: a review, *Energy Fuels*, 2005, **19**, 2098–2106.

4 J. M. Ogden, M. M. Steinbugler and T. G. Kreutz, Comparison of hydrogen, methanol and gasoline as fuels for fuel cell vehicles: implications for vehicle design and infrastructure development, *J. Power Sources*, 1999, **79**, 143–168.

5 H. S. Pajaie, Hydrogen Production from Methanol Steam Reforming over $Cu/ZnO/Al_2O_3/CeO_2/ZrO_2$ Nanocatalyst in an Adiabatic Fixed-Bed Reactor, *Iran. J. Energy Environ.*, 2012, **3**(4), 307–313.

6 T. W. Chiu, R. T. Hong, B. S. Yu, Y. H. Huang, S. Kameoka, A.-P. Tsai, *et al.*, Improving steam-reforming performance by nanopowdering $CuCrO_2$, *Int. J. Hydrogen Energy*, 2014, **39**, 14222–14226.

7 S. Sa, H. Silva, L. Brandao, J. M. Sousa and A. Mendes, Catalysts for methanol steam reforming-a review, *Appl. Catal., B*, 2010, **99**, 43–57.

8 W. H. Cheng, Development of methanol decomposition catalysts for production of H_2 and CO, *Acc. Chem. Res.*, 1999, **32**, 685–691.

9 D. R. Palo, R. A. Dagle and J. D. Holladay, Methanol steam reforming for hydrogen production, *Chem. Rev.*, 2007, **107**, 3992–4021.

10 L. J. Pettersson and R. Westerholm, State of the art of multi-fuel reformers for fuel cell vehicles: problem identification and research needs, *Int. J. Hydrogen Energy*, 2001, **26**, 243–264.

11 J. Agrell, H. Birgersson and M. Boutonnet, Steam reforming of methanol over a $Cu/ZnO/Al_2O_3$ catalyst: a kinetic analysis and strategies for suppression of CO formation, *J. Power Sources*, 2002, **106**, 249–257.

12 N. Itoh, Y. Kaneko and A. Igarashi, Efficient hydrogen production via methanol steam reforming by preventing back permeation of hydrogen in a palladium membrane reactor, *Ind. Eng. Chem. Res.*, 2002, **41**, 4702–4706.

13 R. Y. Abrokwah, V. G. Deshmane, S. L. Owen and D. Kuila, Cu-Ni Nanocatalysts in Mesoporous MCM-41 and TiO_2 to Produce Hydrogen for Fuel Cells via Steam Reforming Reactions, *Adv. Mater. Res.*, 2015, **1096**, 161–168.

14 R. M. Navarro, M. A. Pena and J. L. G. Fierro, Production of Hydrogen by Partial Oxidation of Methanol over a Cu/ZnO/Al_2O_3 Catalyst: Influence of the Initial State of the Catalyst on the Start-Up Behaviour of the Reformer, *J. Catal.*, 2002, **212**, 112–118.

15 B. Lindstrom, L. J. Pettersson and P. Govind Menon, Activity and characterization of Cu/Zn, Cu/Cr and Cu/Zr on γ-alumina for methanol reforming for fuel cell vehicles, *Appl. Catal., A*, 2002, **234**, 111–125.

16 R. Shokrani, M. Haghighi, H. Ajamein and M. Abdollahifar, Hybrid sonochemic urea-nitrate combustion preparation of CuO/ZnO/Al$_2$O$_3$ nanocatalyst used in fuel cell-grade hydrogen production from methanol: effect of sonication and fuel/nitrate ratio, *Part. Sci. Technol.*, 2018, **36**, 217–225.

17 A. Basile, A. Parmaliana, S. Tosti, A. Iulianelli, F. Gallucci, C. Espro and J. Spooren, Hydrogen production by methanol steam reforming carried out in membrane reactor on Cu/Zn/Mg-based catalyst, *Catal. Today*, 2008, **137**, 17–22.

18 Y. H. Huang, S. F. Wang, A. P. Tsai and S. Kameoka, Reduction behaviors and catalytic properties for methanol steam reforming of Cu-based spinel compounds CuX$_2$O$_4$ (X = Fe, Mn, Al, La), *Ceram. Int.*, 2014, **40**, 4541–4551.

19 B. Frank, Steam reforming of methanol over copper-containing catalysts: influence of support material on microkinetics, *J. Catal.*, 2007, **40**, 4541–4551.

20 T. Fujitani and J. Nakamura, The chemical modification seen in the Cu/ZnO methanol synthesis catalysts, *Appl. Catal., A*, 2000, **191**, 111–129.

21 N. Takezawa and N. Iwasa, Steam reforming and dehydrogenation of methanol: difference in the catalytic functions of copper and group VIII metals, *Catal. Today*, 1997, **36**, 45–56.

22 L. Ma, D. L. Trimm and M. S. Wainwright, Structural and catalytic promotion of skeletal copper catalysts by zinc and chromium oxides, *Top. Catal.*, 1999, **8**, 271–277.

23 X. Huang, L. Ma and M. S. Wainwright, The influence of Cr, Zn and Co additives on the performance of skeletal copper catalysts for methanol synthesis and related reactions, *Appl. Catal., A*, 2004, **257**, 235–243.

24 M. B. Gawande, Cu and Cu-Based Nanoparticles: Synthesis and Applications in Catalysis, *Chem. Rev.*, 2016, **116**, 3722–3811.

25 D. Xiong, Z. Xu, X. Zeng, W. Zhang, W. Chen, X. Xu, M. Wang and Y. B. Cheng, Hydrothermal synthesis of ultrasmall CuCrO$_2$ nanocrystal alternatives to NiO nanoparticles in efficient p-type dye-sensitized solar cells, *J. Mater. Chem.*, 2012, **22**, 24760.

26 S. Zhou, X. Fang, Z. Deng, D. Li, W. Dong, R. Tao, G. Meng, T. Wang and X. Zhu, Hydrothermal synthesis and characterization of CuCrO$_2$ laminar nanocrystals, *J. Cryst. Growth*, 2008, **310**, 5375.

27 M. Taghizadeh, H. Akhoundzadeh, A. Rezayan and M. Sadeghian, Excellent catalytic performance of 3D-mesoporous KIT-6 supported Cu and Ce nanoparticles in methanol steam reforming, *Int. J. Hydrogen Energy*, 2018, **43**, 10926–10937.

28 A. Iulianelli, T. Longo and A. Basile, Methanol steam reforming reaction in a Pd–Ag membrane reactor for CO-free hydrogen production, *Int. J. Hydrogen Energy*, 2008, **33**, 5583–5588.

29 B. Y. Hwang, S. Sakthinathan and T. W. Chiu, Production of hydrogen from steam reforming of methanol carried out by self-combusted CuCr$_{1-x}$Fe$_x$O$_2$ (x = 0–1) nanopowders catalyst, *Int. J. Hydrogen Energy*, 2019, **44**, 2848–2856.

30 T. W. Chiu, B. S. Yu, Y. R. Wang, K. T. Chen and Y. T. Lin, Synthesis of nanosized CuCrO$_2$ porous powders via a self-combustion glycine nitrate process, *J. Alloys Compd.*, 2011, **509**, 2933–2935.

31 S. Kameoka, M. Okada and A. P. Tsai, Preparation of a novel copper catalyst in terms of the immiscible interaction between copper and chromium, *Catal. Lett.*, 2008, **120**, 252–256.